Supplementary materials for this article are available at 10.1007/s13253-016-0244-7.

Estimability Analysis and Optimal Design in Dynamic Multi-scale Models of Cardiac Electrophysiology

Matthew S. SHOTWELL and Richard A. GRAY

We present an applied approach to optimal experimental design and estimability analysis for mechanistic models of cardiac electrophysiology, by extending and improving on existing computational and graphical methods. These models are 'multi-scale' in the sense that the modeled phenomena occur over multiple spatio-temporal scales (e.g., single cell vs. whole heart). As a consequence, empirical observations of multi-scale phenomena often require multiple distinct experimental procedures. We discuss the use of conventional optimal design criteria (e.g., D-optimality) in combining experimental observations across multiple scales and multiple experimental modalities. In addition, we present an improved 'sensitivity plot'—a graphical assessment of parameter estimability—that overcomes a well-known limitation in this context. These techniques are demonstrated using a working Hodgkin–Huxley cell model and three simulated experimental procedures: single-cell stimulation, action potential propagation, and voltage clamp. In light of these assessments, we discuss two model modifications that improve parameter estimability, and show that the choice of optimality criterion has a profound effect on the contribution of each experiment.
Supplementary materials accompanying this paper appear on-line.

Key Words: Cardiac cell model; Identifiability; Sensitivity plot; Voltage clamp.

1. INTRODUCTION

Multi-scale methods are used to study phenomena that occur over multiple temporal or spatial scales (Hunter and Borg 2003), and observations at different scales often require distinct experimental procedures. Human physiological processes are inherently multi-scale, as the human body coordinates the transfer of "information" across a wide range of spatial and temporal scales. No single model is yet capable of reproducing this hierarchy, and one of the biggest outstanding problems in quantitative physiology is to develop the methodology

Matthew S. Shotwell (✉) Department of Biostatistics, Vanderbilt University, 2525 West End Ave., Nashville, TN 37203, USA. Richard A. Gray, Center for Devices and Radiological Health, Food and Drug Administration, Silver Spring, MD, USA (E-mail: *matt.shotwell@vanderbilt.edu*).

Journal of Agricultural, Biological, and Environmental Statistics
DOI: 10.1007/s13253-016-0244-7

Published online: 21 January 2016

for simultaneous modeling and assessment of data that arise from multiple, multi-scale experimental frameworks.

Multi-scale models can be constructed by combining single-scale models (Ingram et al. 2004), which increase the model complexity in terms of the number and relationships among model parameters. Indeed, electrophysiological models are often overparameterized (Fink and Noble 2009). Thus, in developing multi-scale models, it is helpful to characterize the relationships between the model parameters and model outputs. Specifically, if there are multiple parameter values that render identical model output, then the parameters cannot be uniquely identified given model output, nor estimated using empirical observations.

Even when the parameters are estimable, there can be considerable statistical uncertainty. However, by studying the model, experiments can be designed to reduce uncertainty. In the case of multi-scale models, where there are distinct experimental procedures that give rise to observations at each scale, it can also be helpful to compare the relative degree of information associated with each type of experiment, and thereby focus limited resources on the most informative experiments.

In this article, we present a practical and general computational and graphical approach to estimability assessment and optimal experimental design in the context of multi-scale models. These methods are demonstrated using a working Hodgkin–Huxley model of the mammalian cardiac excitable cell and three simulated experimental procedures that are commonly used to study these cells (Hodgkin and Huxley 1952). The three experimental procedures are as follows: single-cell excitation that produces an all-or-none action potential, action potential propagation along a fiber or 'cable' of electrically connected cells (Joyner et al. 1991), and a voltage clamp experiment designed to study the voltage-gated Na^+ channel (Berecki et al. 2010), which is primarily responsible for the initiation of an action potential. In light of these assessments, we discuss two model modifications that improve parameter estimability, and show that the choice of optimality criterion has a profound effect on the contribution of each experiment. In order to facilitate the ensuing discussion, and to promote the future use of these methods, we have created an on-line supplement of `R` computer code that is referenced throughout the article as the "Code Supplement."

2. BACKGROUND

The methods and techniques associated with nonlinear model identifiability, parameter estimability, optimal experimental design, and their association are well studied (Rothenberg 1971; Jacquez and Greif 1985; Walter and Pronzato 1996). In related fields, parameter estimation is sometimes called the "inversion problem." The conditions under which inversion is possible have been studied in the context of single current voltage clamp models (Wang and Beaumont 2004; Lee et al. 2006; Csercsik et al. 2012; Raba et al. 2013). In contrast, we present a generic approach that has applications beyond excitable cell models, and that incorporates multiple, multi-scale experimental frameworks to simultaneously solve the inversion problem.

2.1. MODEL IDENTIFIABILITY

Let $\eta(x,\theta) = [\eta_1(x,\theta)\ldots\eta_m(x,\theta)]^T$ represent the m-variate response of an experimental system under condition x, given p-variate parameter θ. The experimental condition x may be arbitrarily structured, depending on the nature of the experiment. For example, consider a pharmacokinetic model for the concentration of drug after intravenous infusion. The experimental condition variable might simultaneously represent the time relative to infusion, initial drug concentration, and the rate and duration of infusion.

The model given by $\eta(x,\theta)$ is *identifiable* if and only if $\eta(\cdot,\theta) = \eta(\cdot,\theta')$ implies $\theta = \theta'$ for all possible θ (Rothenberg 1971). Or in words, if the response function at θ is identical to that at θ', then θ' must equal θ, for all possible θ. Otherwise the model is not identifiable. Thus, identifiability can be difficult to establish, since all possible parameter values must be considered. However, in many applications, it is sufficient to *localize* the analysis of model identifiability to a region of plausible parameter values. A model is *locally identifiable* at θ' if the foregoing implication holds for θ in a neighborhood of θ', which suggests that the problem can be analyzed by linearization of $\eta(x,\theta)$ about θ'. The first-order Taylor series approximation of $\eta(x,\theta)$ in a neighborhood of θ' is

$$\eta(x,\theta) \approx \eta\left(x,\theta'\right) + J\left(x,\theta'\right)\left(\theta' - \theta\right), \tag{1}$$

where the elements of the Jacobian $J(x,\theta')$ are

$$J\left(x,\theta'\right)_{i,j} = \left[\frac{\partial\eta_i(x,\theta)}{\partial\theta_j}\right]_{\theta=\theta'} \tag{2}$$

for $i = 1,\ldots m$ and $j = 1,\ldots,p$. Thus, locally identifiability is verified when, for some experimental condition x, there are no nontrivial solutions (i.e., $\theta \neq \theta'$) to the following linear system

$$J\left(x,\theta'\right)\left(\theta' - \theta\right) = 0. \tag{3}$$

By definition, this requires linear independence in the columns of $J(x,\theta')$. However, in most cases no single experiment is sufficient to satisfy the criterion for local identifiability. Local identifiability can then be verified by searching for two or more experiments that jointly ensure no nontrivial solutions to an expanded linear system

$$\boldsymbol{J}\left(\boldsymbol{x},\theta'\right)\left(\theta' - \theta\right) = \mathbf{0}, \tag{4}$$

where $\boldsymbol{J}(\boldsymbol{x},\theta')$ is an $nm \times p$ matrix consisting of n blocks of $m \times p$ Jacobians (expression 2), and $\boldsymbol{x}$ are the n associated experimental conditions. Local identifiability about θ' is then assessed by verification of columnwise linear independence in $\boldsymbol{J}(\boldsymbol{x},\theta')$, or equivalently that $M(\boldsymbol{x},\theta') = \boldsymbol{J}(\boldsymbol{x},\theta')^T\boldsymbol{J}(\boldsymbol{x},\theta')$ is nonsingular. The matrices $\boldsymbol{J}(\boldsymbol{x},\theta')$ and $M(\boldsymbol{x},\theta')$ are, respectively, the *sensitivity matrix* and *information matrix* associated with the collection of experimental conditions $\boldsymbol{x}$. Also note that the information matrix can be written as the sum $\sum_{i=1}^{n}\mu(x_i,\theta')$, where $\mu(x_i,\theta') = J(x_i,\theta')^T J(x_i,\theta')$ is the information contribution of condition x_i.

Grewal and Glover (1976) showed that local identifiability of a linearized model is sufficient, but not necessary, to demonstrate local identifiability of the corresponding nonlinear model. This has generated interest in alternative criteria and tests for local identifiability (e.g., Hengl et al. 2007; Raue et al. 2009; Kim and Lindsay 2014). However, identifiability of the linearized model remains an important requirement for many types of nonlinear optimization methods, as we demonstrate below for the nonlinear least-squares method.

2.2. PARAMETER ESTIMABILITY

Parameter estimability is related to identifiability, but is conditional on a specific experimental design. Specifically, model parameters are considered locally estimable under experimental design $\boldsymbol{x}$, when $\boldsymbol{x}$ is sufficient for local identifiability. To further illustrate the connection, consider the statistical model

$$\boldsymbol{y} = \boldsymbol{\eta}(\boldsymbol{x}, \theta) + \boldsymbol{\epsilon}, \tag{5}$$

where $\boldsymbol{y}$ is an $nm \times 1$ vector of observations on responses $\boldsymbol{\eta}(\boldsymbol{x}, \theta)$ in a series of n experiments $\boldsymbol{x}$, and $\boldsymbol{\epsilon}$ represents a vector of random errors. For simplicity, we assume that the errors are independent and homoscedastic with mean zero and variance σ^2. The nonlinear least-squares (NLS) estimate for θ satisfies the estimating equations $\boldsymbol{J}(\boldsymbol{x}, \hat{\theta})^T[\boldsymbol{y} - \boldsymbol{\eta}(\boldsymbol{x}, \hat{\theta})] = \boldsymbol{0}$. Substituting expression (1) renders the linearized NLS estimating equations

$$M(\boldsymbol{x}, \theta')\big(\hat{\theta} - \theta'\big) = \boldsymbol{J}\big(\boldsymbol{x}, \theta'\big)^T \big[\boldsymbol{y} - \boldsymbol{\eta}\big(\boldsymbol{x}, \theta'\big)\big]. \tag{6}$$

The solution to (6) is unique when $M(\boldsymbol{x}, \theta')$ is nonsingular, or equivalently when θ is locally estimable at θ'. Expression (6) motivates an iterative Newton–Raphson solution for the NLS estimating equations

$$\hat{\theta}_{s+1} = \hat{\theta}_s + M\big(\boldsymbol{x}, \hat{\theta}_s\big)^{-1} \boldsymbol{J}\big(\boldsymbol{x}, \hat{\theta}_s\big)^T \Big[\boldsymbol{y} - \boldsymbol{\eta}\big(\boldsymbol{x}, \hat{\theta}_s\big)\Big], \tag{7}$$

In order to evaluate the algorithm at each iteration, $M(\boldsymbol{x}, \hat{\theta}_s)$ must be nonsingular, and thus θ must be locally estimable at $\hat{\theta}_s$. This demonstrates that local identifiability of the linearized model is an important computational feature, although unnecessary for local identifiability of the corresponding nonlinear model.

2.3. OPTIMAL EXPERIMENTAL DESIGN

Even when the criterion for parameter estimability is satisfied, parameter estimates may be highly variable, or otherwise *ill-conditioned*. For NLS estimators, the information matrix $M(\boldsymbol{x}, \theta)$ determines the conditioning of the estimation problem. For instance, the approximate variance of the NLS estimate is

$$V[\hat{\theta}] = \sigma^2 M\big(\boldsymbol{x}, \hat{\theta}\big)^{-1}. \tag{8}$$

The conditioning of an estimation problem can be assessed using a variety of criteria. One such criterion is the matrix condition number. For a linear system $AX = C$, the condition number of A is equal to $||A||||A^{-1}||$, where $||A||$ is matrix norm. The condition number represents the maximum relative change in $||X||$ induced by a one-unit relative change in $||C||$. Specifically,

$$\frac{||\Delta X||}{||X||} \leq ||A||\left|\left|A^{-1}\right|\right|\frac{||\Delta C||}{||C||}, \tag{9}$$

where ΔX is the change in X that results from a change ΔC in C. When $||A||$ is the induced 2-norm (i.e., the largest Euclidean norm $||Ax||$ where x is a unit vector), the condition number is identical to the ratio of the maximum and minimum eigenvalues of A. Thus, the condition number can take values greater than or equal to one. An estimation problem is ill-conditioned when the condition number of the information matrix is large, and well conditioned when the condition number is near one. The reciprocal of the condition number (RCN), of course, has the reciprocal interpretation. Experimental designs that maximize the RCN of the information matrix are called K-optimal (Rempel and Zhou 2014). Thus, the condition number is called the K-optimality criterion.

The determinant of the information matrix is also indicative of ill-conditioned estimation problems, and has an intuitive interpretation. Specifically, the NLS estimate $\hat{\theta}$ has an approximate normal distribution, such that the volume of the confidence ellipsoid for θ is inversely related to the determinant of the information matrix. Thus, experiments that minimize the determinant of $M(\boldsymbol{x}, \hat{\theta})^{-1}$ also minimize the confidence ellipsoid volume. Such designs are called D-optimal, and $|M(\boldsymbol{x}, \hat{\theta})^{-1}|$ is the D-optimality criterion (Fedorov and Leonov 2013).

The related E-optimality criterion is the reciprocal of the minimum eigenvalue of the information matrix. Thus, minimizing the E-optimality criterion is equivalent to minimizing the largest diameter (principle axis) of the confidence ellipsoid.

A fourth criterion, the A-optimality criterion can be used to isolate uncertainty about one or more parameters: $\text{tr}[AM(\boldsymbol{x}, \theta)^{-1}]$, where A is a square nonnegative definite matrix and $\text{tr}[\cdot]$ represents the matrix trace. For example, when $A = I$, where I is the $p \times p$ identity matrix, the A-optimality criterion is proportional to the average approximate variance among the elements of $\hat{\theta}$.

3. MULTI-SCALE ESTIMABILITY AND OPTIMAL DESIGN

The experimental frameworks that inform multi-scale models of cardiac electrophysiology often require significant preparation, but can yield information under a rich array of experimental conditions. For example, the cost of each test voltage in a voltage clamp experiment is relatively minor in comparison to the effort of preparing the experiment. Thus, the cost of experimentation is "front loaded," whereas in other experimental frameworks, for example human pharmacokinetic studies, the cost is more evenly distributed across the experimental conditions.

The notion of "front loaded" cost is exacerbated in multi-scale models, since observations at different scales often require different experimental frameworks. Hence, in designing

collections of experiments to inform such models, there may be less interest in optimizing within-experiment design aspects (e.g., the count and spacing of test voltages), and more interest on the types and frequency of whole experiments, although the former is also amenable to optimal design. Similarly, in assessments of parameter estimability, the modeler may be more interested in the types of experiments that are necessary to simultaneously estimate the model parameters.

The following discussion illustrates these unique multi-scale aspects of estimability and optimal design using a simplified Hodgkin–Huxley model of the cardiac action potential, and three distinct experimental modalities, which represent three distinct spatio-temporal scales.

4. CARDIAC CELL MODEL

Dynamic models of cardiac electrophysiology are used to study the behavior of cardiac tissue under pathological and therapeutic perturbations (e.g., arrhythmias and defibrillation, respectively). The model presented below is a modification of the well-known Hodgkin–Huxley (Hodgkin and Huxley 1952) model of nerve conduction and excitation, that retains a detailed characterization of Na^+ channel kinetics, which is primarily responsible for rapid depolarization during the cardiac action potential. The simplified model is a system of partial differential equations in time t, and one dimension of space z, which represents an electrically conductive fiber of cardiac cells. The model equations are as follows:

$$\begin{aligned} C_m \frac{\partial V}{\partial t} &= -I_{\text{ion}} - I_{\text{stim}} - C_m D \frac{\partial^2 V}{\partial z^2} \\ \frac{\partial m}{\partial t} &= (m_\infty - m)/\tau_m \\ \frac{\partial h}{\partial t} &= (h_\infty - h)/\tau_h, \end{aligned} \tag{10}$$

where V represents transmembrane voltage, I_{ion} is the transmembrane current resulting from the flux of Na^+ and K^+ ions through voltage-gated ion channels:

$$I_{\text{ion}} = g_{\text{Na}} m^3 h \big(V - E_{\text{Na}}\big) + g_{\text{K}} \big(V - E_{\text{K}}\big) e^{-(V - E_K)/k_r}. \tag{11}$$

The variables m and h are gating variables that, respectively, characterize the voltage-dependent activation and inactivation of transmembrane Na^+ channels. I_{stim} is an externally applied stimulus current, and $D\frac{\partial^2 V}{\partial z^2}$ represents the diffusion of charge along the tissue fiber. The voltage dependence of m, h, and τ_h is expressed as follows:

$$\begin{aligned} m_\infty &= \left[1 + e^{-(V - E_m)/k_m}\right]^{-1} \\ h_\infty &= \left[1 + e^{-(V - E_h)/k_h}\right]^{-1} \\ \tau_h &= 2\tau_{h0} \left[e^{-\delta_h (V - E_m)/k_m} + e^{(1-\delta_h)(V - E_m)/k_m}\right]^{-1}. \end{aligned} \tag{12}$$

Table 1. Parameter values and descriptions.

Parameter	Value	Units	Description
C_m	–	μF·cm^{-2}	Membrane capacitance
g_{Na}	11.00	mS·cm^{-2}	Na^+ channel maximum conductance
E_{Na}	65.00	mV	Na^+ channel Nernst reversal potential
g_{K}	0.30	mS·cm^{-2}	K^+ channel maximum conductance
E_{K}	−83.00	mV	K^+ channel Nernst reversal potential
k_r	21.28	mV	K^+ channel nonlinearity
D	0.001	cm^2·ms^{-1}	Diffusion coefficient
E_m	−41.00	mV	Na^+ channel half-activation voltage
k_m	4.00	mV	Na^+ channel activation slope
τ_m	0.12	ms	Na^+ channel activation time constant
E_h	−74.70	mV	Na^+ channel half-inactivation voltage
k_h	−4.40	mV	Na^+ channel inactivation slope
τ_{h0}	6.81	ms	Na^+ channel inactivation time constant scale
δ_h	0.80	–	Na^+ channel inactivation time constant asymmetry

The dimension "mS" represents millisiemens, the Standard International (SI) unit for electrical conductance. One siemens is equal to the reciprocal of one ohm, the SI unit for electrical resistance. In notation $S = \Omega^{-1}$.

The parameter C_m represents membrane capacitance, which scales the transmembrane voltage V. We treat this parameter as fixed, and interpret V relative to membrane capacitance. Thus, the model has thirteen free parameters, collectively denoted θ, which are listed in Table 1. The parameter values were selected to be consistent with experimental results in rabbits (Gray et al. 2013).

The model solutions can be used to make predictions about the behavior of cardiac tissue under a variety of experimental conditions. Specifically, the cell model exhibits a stable quiescent steady state in which the cell is capable of "excitation" via external stimulus, which results in an all-or-none action potential; a rapid change in transmembrane potential that plateaus for a period of time and subsequently returns to quiescent state (see model output V in Fig. 1). Adjacent cells can be excited by the neighboring action potential, thereby propagating the action potential along a fiber. The transmembrane potential can also be experimentally manipulated in order to investigate the transmembrane currents that give rise to an action potential. The following three subsections describe three such experimental frameworks that were simulated to examine model behavior at three distinct spatio-temporal scales.

4.1. SINGLE-CELL STIMULATION

Single-cell stimulation experiments were modeled by prohibiting charge diffusion along the tissue fiber (i.e., by setting parameter $D = 0$). Given the parameter values listed in Table 1, initial values $V = -83$, $m = m_\infty$, and $h = h_\infty$, and a stimulus perturbation I_{stim}, the solutions of Eqs. (10) were approximated using first-order Euler numerical integration (Code Supplement Section 2). Figure 1 illustrates the single-cell solution given a smoothed square-wave stimulus. The figure is separated into two columns, where the left-hand panels represent the depolarization phase and the right-hand panels represent repolarization. The

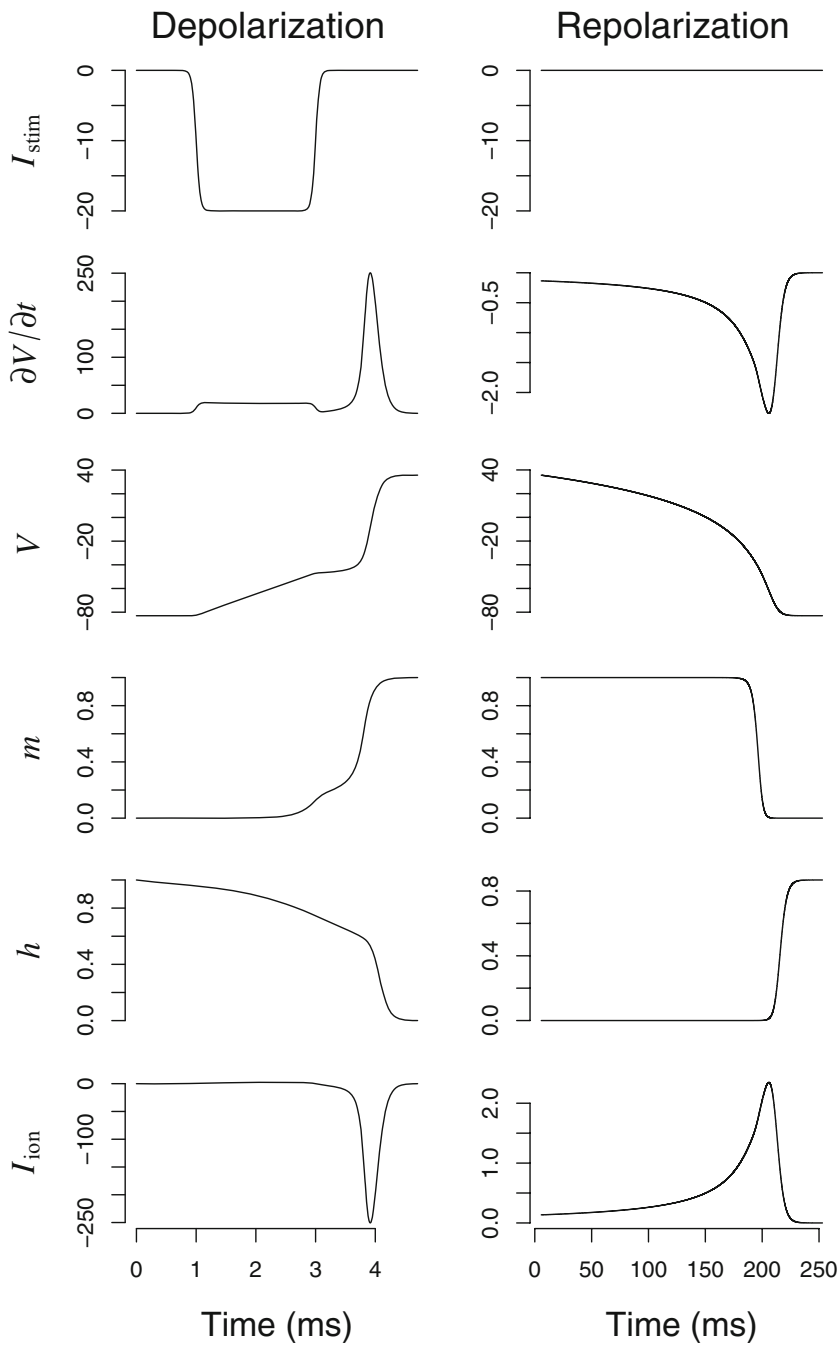

Figure 1. Single-cell solution for Eqs. (10), (11), and (12). A smoothed *square-shaped* stimulus current was applied over two ms (*top-left panel*).

two phases are plotted separately, since depolarization occurs over a much shorter time scale and is associated with much larger transmembrane currents.

4.2. ACTION POTENTIAL PROPAGATION

A four centimeter fiber of tissue was simulated to examine action potential behavior under propagation conditions. One millimeter of the fiber terminus was stimulated by holding the transmembrane potential at zero (via I_{stim}) for two milliseconds, which induced a propagating action potential. Each of the model outputs were then recorded at the midpoint of the fiber (2cm; Code Supplement Section 3). Web Figure 1 illustrates the midpoint solution, where $I_D = D\partial^2 V/\partial z^2$ is plotted instead of I_{stim}, since the stimulus for the fiber midpoint arises from neighboring tissue.

4.3. Na^+ CHANNEL INACTIVATION VOLTAGE CLAMP

Voltage clamp experiments are designed to isolate the time- and voltage-dependence of transmembrane currents by experimentally "clamping" the transmembrane potential at specified voltages and measuring the resultant currents. A voltage clamp *protocol* comprises a sequence of clamp voltages and the durations of each clamp. Protocols are designed to elucidate the kinetics of particular transmembrane currents.

In the cardiac cell, voltage-gated Na^+ channels are activated by a depolarization stimulus, which causes further rapid depolarization due to the influx of Na^+ ions. The Na^+ channel then becomes inactivated. The kinetics of Na^+ channel inactivation can be studied using a voltage clamp protocol consisting of *conditioning*, *pre-test*, and *test* pulse triplets. The conditioning pulse (-140 mV) remains constant in each triplet, and is held for a duration (1 s) that ensures the cell has recovered from inactivation. The pre-test pulse is variable (-140 mV to 0 mV in 5 mV steps), and is held for a duration (1 s) that is sufficient to achieve a certain degree of steady-state inactivation. The subsequent test pulse (-20 mV for 20 ms) causes Na^+ channel activation, which is attenuated by the degree of inactivation induced by the pre-test pulse. The degree of attenuation in the peak current following each test pulse is used as a measure of steady-state inactivation. Steady-state Na^+ channel inactivation exhibits a sigmoidal shape as a function of conditioning voltage, which is modeled using the parametric sigmoidal function h_∞ (12). See Berecki et al. (2010) for additional details. This protocol was simulated by fixing the transmembrane potential at the appropriate levels and times (Code Supplement Section 4).

4.4. STATISTICAL FRAMEWORK

In the action potential propagation and single-cell experiments, ion current I_{ion} is reported as a function of transmembrane potential V separately during the depolarization and repolarization phases, since the I_{ion} versus V relationship exhibits hysteresis across these phases. For the Na^+ channel inactivation experiments, the maximum ion current following each test pulse is reported as a function of the pre-test voltage. Because ion current is the only

observed response, we employ a univariate version of model (5) as the basis for assessments of identifiability and optimal design:

$$\boldsymbol{y} = \eta(\boldsymbol{v}, \boldsymbol{x}, \theta) + \boldsymbol{\epsilon}, \tag{13}$$

where $\boldsymbol{y}$ is a vector of measured currents at (conditioning) voltages $\boldsymbol{v}$, under experimental conditions $\boldsymbol{x}$. In this context, each element of $\boldsymbol{x}$ represents the type of experiment. Thus, as in expression (5), the model outputs are "stacked" into a single vector. The assumption of homoscedastic and independent errors is approximate, but can be relaxed using general nonlinear least-squares or likelihood methods.

In the computer code implementation, the function η is approximated by interpolating (with natural cubic splines) the time solutions for V and I_{ion}, which are computed by first-order Euler numerical integration (Code Supplement Sections 2, 3, and 4). The sensitivity matrices were computed using numerical differentiation in a similar fashion.

Each type of experiment gives rise to a series of current measurements, which are sampled as a function of voltage. Since we are concerned with identifiability and optimal design at the whole experiment level, we denote the sensitivity and information matrices associated with the single-cell, action potential propagation, and Na^+ channel inactivation voltage clamp experiments as $\boldsymbol{J}_{0\text{D}}$, $\boldsymbol{J}_{1\text{D}}$, $\boldsymbol{J}_{\text{VC}}$, and $M_{0\text{D}}$, $M_{1\text{D}}$, M_{VC}, respectively, where it is understood that each is conditional on the corresponding subsets of $\boldsymbol{v}, \boldsymbol{x}$, and the model parameter vector θ. Thus, the information matrix for each experiment is computed by substituting $\eta(\boldsymbol{v}, \boldsymbol{x}, \theta)$ for $\eta(\boldsymbol{x}, \theta)$ in the Jacobian expressions 2, 3, and 4. See Web Appendix B for an explicit expression for the information matrix.

The single-cell and action potential propagation experiments are further separated by depolarization and repolarization phases, which are denoted with subscripts 0Dr and 0Dd, respectively. The pooled information matrix, which represents the combined information from each type of experiment, is expressed as a weighted sum of the experiment-specific information matrices as follows:

$$M_{\text{pool}} = w_{0\text{Dr}} M_{0\text{Dr}} + w_{0\text{Dd}} M_{0\text{Dd}} + w_{1\text{Dr}} M_{1\text{Dr}} + w_{1\text{Dd}} M_{1\text{Dd}} + w_{\text{VC}} M_{\text{VC}}. \tag{14}$$

The weights in expression (14) are nonnegative scalar quantities that sum to one, and represent the relative contribution of each type of experiment. The weights can be considered the relative amounts of "effort" allocated to each type of experiment, or can be used in a weighted estimation procedure. The pooled information matrix can be equivalently expressed in terms of the weighted experiment-specific sensitivity matrices, e.g., $M_{\text{pool}} = \boldsymbol{J}^T \boldsymbol{J}$ where $\boldsymbol{J}$ is the weighted sensitivity matrix

$$\boldsymbol{J} = \left[\sqrt{w_{0\text{Dr}}}\, \boldsymbol{J}_{0\text{Dr}}, \sqrt{w_{0\text{Dd}}}\, \boldsymbol{J}_{0\text{Dd}}, \sqrt{w_{1\text{Dr}}}\, \boldsymbol{J}_{1\text{Dr}}, \sqrt{w_{1\text{Dd}}}\, \boldsymbol{J}_{1\text{Dd}}, \sqrt{w_{\text{VC}}}\, \boldsymbol{J}_{\text{VC}}\right].^T \tag{15}$$

The weights can then be selected to achieve optimality with respect to an optimal design criterion on the pooled information matrix.

For the D-, E-, and A-optimality criteria, and under certain regularity conditions, the optimization problem is convex and can be implemented using a simple gradient-descent

Table 2. The K-, D-, E-, and A-efficient weights for each type of experiment and the reciprocal condition number (RCN) of the corresponding pooled information matrix.

Weight	K-optimal	D-optimal	E-optimal	A-optimal
RCN	1.13×10^{-8}	1.05×10^{-10}	4.48×10^{-9}	1.76×10^{-9}
w_{0Dd}	5.4×10^{-4}	3.1×10^{-1}	1.2×10^{-1}	2.1×10^{-1}
w_{1Dd}	8.9×10^{-5}	3.9×10^{-1}	4.1×10^{-2}	1.0×10^{-1}
w_{0Dr}	4.9×10^{-1}	1.0×10^{-5}	8.3×10^{-7}	1.0×10^{-5}
w_{1Dr}	5.1×10^{-1}	1.0×10^{-5}	8.1×10^{-1}	6.2×10^{-1}
w_{VC}	3.9×10^{-4}	3.0×10^{-1}	2.2×10^{-2}	7.3×10^{-2}

method (Fedorov and Leonov 2013). The K-optimality criterion is not convex, and not necessarily smooth. To account for this, we used 10^5 random initializations of the study weights, followed by numerical gradient-descent. The random initialization step is equivalent to nonadaptive stochastic search (NASS). The algorithm details are provided in Web Appendix A. Implementation details are provided in Code Supplement Section 5.

4.5. COMPUTATIONAL ESTIMABILITY AND EFFICIENCY ASSESSMENT

The reciprocal condition number (RCN) for each experiment-specific information matrix was equal to zero or less than "double" floating-point precision (approximately 2.2×10^{-16}), indicating that no single experiment is sufficient to simultaneously estimate the 13 free model parameters (see Table 1). However, the current diffusion parameter D is experimentally fixed in the single-cell and voltage clamp experiments. Excluding this parameter, the RCN for the pooled single-cell information matrices ($w_{0Dr} = w_{0Dd} = 1/2$) was 3.98×10^{-14}, which indicates that the 12 remaining parameters are weakly estimable using data that arise from single-cell experiments.

Combining the single-cell, action potential propagation, and inactivation voltage clamp experiments with equal weights improved the RCN of the pooled information by more than seven orders of magnitude (6.94×10^{-10}), relative to the largest RCN associated with any individual experiment (2.40×10^{-18} for the action potential propagation experiment). Thus, by pooling information across the three types of experiment, the 13 model parameters are simultaneously estimable. However, in this scenario, some of the parameter estimates are highly correlated (cf. expression 8). The largest correlation, 0.995, occurs between parameter estimates for δ_h and k_h.

The K-, D-, E-, and A-efficient weights (where $A = I$) for each of the experiments are listed in Table 2. The RCN of the K-efficient design was improved by more than two orders of magnitude (1.13×10^{-8}), relative to the equal-weighted design. The largest correlation between any two parameter estimates, again for δ_h and k_h, was reduced to 0.985. The RCN for the D- and A-efficient designs were 1.05×10^{-10} and 1.76×10^{-9}, respectively.

4.6. GRAPHICAL ESTIMABILITY AND EFFICIENCY ASSESSMENT

The *sensitivity plot* (McLean and McAuley 2012) is a graphical technique to aid in the assessment of estimability and design efficiency, by examining the weighted model sensi-

tivity matrix (e.g., expression 15). The sensitivity values are graphically arranged according to model parameter, so that their linear dependencies are more easily visualized.

The sensitivity plot is suitable for models with few parameters, but scales poorly as dependencies become increasingly difficult to visualize. Furthermore, the sensitivity plot does not directly convey information regarding the conditioning of estimation problems. In order to overcome these limitations, we present an augmented sensitivity plot that utilizes shading to indicate the degree of linear dependence among the weighted sensitivities, and thus the design efficiency.

For each parameter, the shading intensity represents the fraction variability in the corresponding sensitivities that cannot be explained by a linear combination of sensitivities for the remaining parameters. Thus, the shading intensity is a measure of linear independence. Lighter shading indicates greater dependence, reduced estimability, greater correlation among parameter estimates, and poor conditioning of the information matrix. When no shading is visible, the parameters are not estimable, or weakly estimable. Specifically, for each parameter indexed by k, the shading intensity is computed as follows: $s_k = 1 - (\boldsymbol{e}_k^T \boldsymbol{e}_k / \boldsymbol{J}_k^T \boldsymbol{J}_k)^r$, where $\boldsymbol{e}_k = \boldsymbol{J}_k - \boldsymbol{J}_{\not k}(\boldsymbol{J}_{\not k}^T \boldsymbol{J}_{\not k})^- \boldsymbol{J}_{\not k}^T \boldsymbol{J}_k$ and r is a graphical tuning parameter that scales the shading intensity ($r = 10$ in the examples). In these expressions, $\boldsymbol{J}_k$ denotes the k^{th} column of the weighted sensitivity matrix $\boldsymbol{J}$, its complement $\boldsymbol{J}_{\not k}$ is a matrix comprising the remaining $p - 1$ columns, and $(\boldsymbol{J}_{\not k}^T \boldsymbol{J}_{\not k})^-$ is the Moore–Penrose generalized inverse of $\boldsymbol{J}_{\not k}^T \boldsymbol{J}_{\not k}$. The rightmost addend of the second expression represents the linear least-squares approximation of $\boldsymbol{J}_k$ given $\boldsymbol{J}_{\not k}$.

Figure (2) is the augmented sensitivity plot for the K-efficient weighted (see Table 2) sensitivity matrix (15), arranged by parameter, transmembrane voltage, and experiment type. The sensitivity plot visually corresponds to the transpose of the weighted sensitivity matrix.

4.7. ALTERNATIVE PARAMETERIZATION

Since the shading for parameters δ_h and k_h is light but detectable in Fig. 2, the graphical and computational assessments are consistent; that parameters δ_h and k_h are only weakly estimable and their estimates are highly correlated. In order to overcome this, an alternative model parameterization was considered.

The voltage-dependent time constants of Na^+ channel activation (τ_m) and inactivation (τ_h) are thought to differ in their scale but have similar shape. In particular, activation is much faster than inactivation (Beaumont et al. 1993). Thus, by expressing τ_m as a fraction of τ_h, we hypothesized that information associated with Na^+ channel activation would aid in estimating the kinetics of inactivation (i.e., δ_h and k_h). In the alternative parameterization, the scalar τ_m was instead set equal to 1/10th of the voltage-dependent τ_h given in expression (12). Hence, both time constants were modeled as proportional, voltage-dependent quantities. This modification had the effect of reducing the correlation between estimates of k_h and δ_h, at the expense of additional correlation among other model parameters, notably g_{Na} and E_{Na} (compare the augmented sensitivity plot in Fig. 2 with Web Figure). The K-efficient RCN of the modified model was improved (increased) by 73%, relative to the original model.

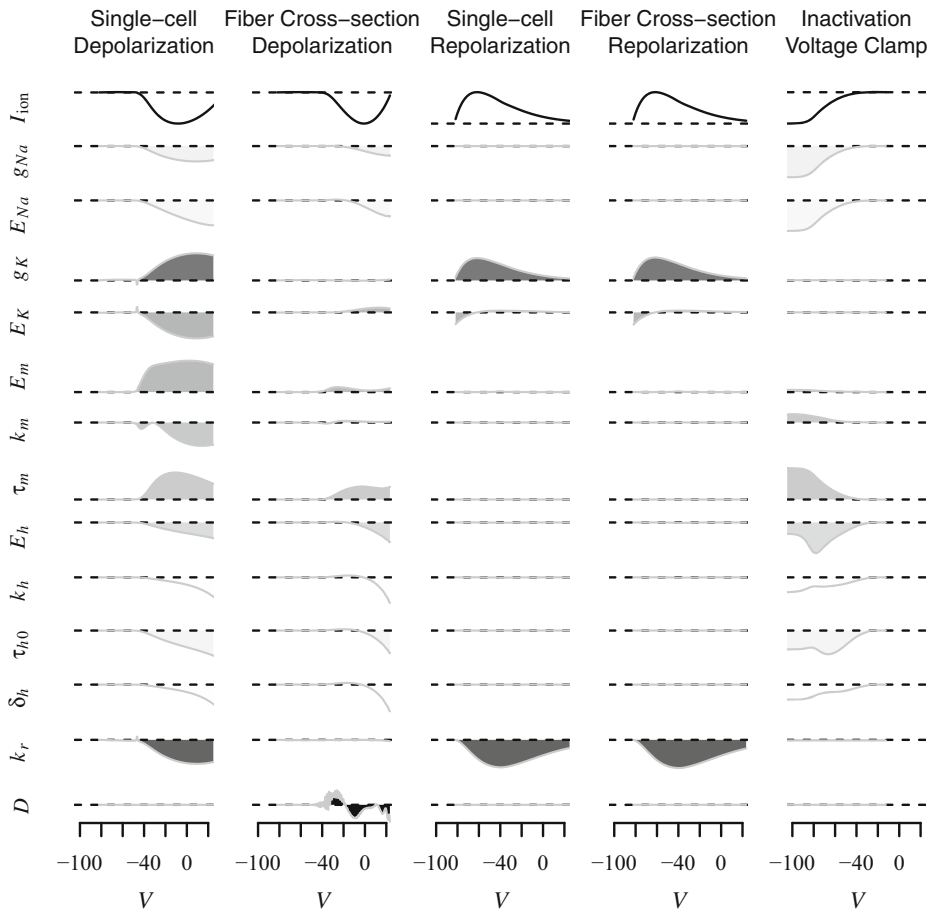

Figure 2. Augmented sensitivity plot for the 13 parameters of the cardiac ion-channel model given by expressions (10), (11), and (12). The uppermost *row* of *panels* plot the model solution (*solid black lines*) for I_{ion} as a function of V during depolarization and repolarization, and in single-cell and fiber midpoint experiments. *Dashed black lines* mark the y-axis origin. *Solid gray lines* represent the sensitivity values for the corresponding parameter and experiment type. In each row of panels, the intensity of the shaded regions is constant, and represents the degree of linear dependence of the corresponding parameter sensitivity values on that of the other parameters. *Lighter shading* indicates greater dependence and reduced identifiability and estimability. When no shading is visible, the model is not estimable, or weakly estimable.

4.8. RESCALING MEMBRANE POTENTIAL AND TIME

Nondimensionalization is a method to identify model parameters that have the sole effect of scaling the model variables. In the modified model of the preceding section, transmembrane potential and time can each be rescaled as follows: $t' = t/t_0$ and $V' = V/V_0$. The tissue fiber position variable (z) can also be rescaled, but we have not done so here. The scale parameters t_0 and V_0 are then selected such that the rescaled model in variables t' and V' has fewer parameters. Specifically, let $t_0 = g_{\text{Na}}^{-1}$ and $V_0 = E_{\text{Na}}$. Substituting these expressions into equations (10), (11), and (12) yields the following simplified expression for I_{ion}:

$$I_{\text{ion}} = m^3 h\left(V' - 1\right) + g'_{\text{K}}\left(V' - E'_{\text{K}}\right)e^{-\left(V' - E'_{\text{K}}\right)/k'_r}, \tag{16}$$

where $g'_{\text{K}} = g_{\text{K}}/g_{\text{Na}}$, $E'_{\text{K}} = E_{\text{K}}/E_{\text{Na}}$, and $k'_r = k_r/E_{\text{Na}}$. Each other model parameter (except δ_h, which is already unitless) is similarly scaled. Indeed, the parameters g_{Na} and E_{Na} only appear as ratios of other parameters. In other words, given the other model parameters, the only effects of E_{Na} and g_{Na} are to scale membrane potential and time, respectively. Thus, by ignoring the scale of membrane potential and time, these two parameters can be fixed for the purposes of identifiability, estimability, and optimal design analyses. Doing so improves the K-efficient RCN by nearly two orders of magnitude, relative to the modified model described in the preceding section (compare Web Figure 2 with Web Figure 3).

5. DISCUSSION

The approaches described above, regarding estimability analysis of an optimal design, are generic and rely on numerical methods to compute model responses and their sensitivities to the model parameters. This is especially satisfactory when there are many alternative models, complex models, or models with many multi-scale outputs. Secondly, the methods we employ are closely tied to the NLS estimation procedure. Indeed, much of the computer code that implements the estimability analysis and optimal design procedures can be reused for the purposes of estimation. For an applied statistician, this continuity may help to conceptualize and implement the process, from estimability analysis and optimal design to eventual parameter estimation using experimental data.

The methods presented herein are not restricted to statistical models with continuous outcome and additive error. More generally, for models that are expressed using a probability model, identifiability implies that no two distinct parameter values render identical probability distributions. The notions of estimability and optimal design are likewise extended by evaluating the likelihood function sensitivities and Fisher information matrix, respectively.

The estimability and optimal design tasks are modular, in the sense that any number of experiments can be considered or omitted. Indeed, the augmented sensitivity plot can be used interactively to consider alternative model parameterizations, and to identify experiments or even conditions within experiments that are most informative about one or more model parameters. This modularity is especially useful in the context of multi-scale phenomena and the associated experimental frameworks, in which the effort is often "front loaded."

The criterion selected for design optimization can have a significant effect on the weighting of experiments, as is evidenced by the weights in Table 2. Although some of the weights are very small, it should not be taken for granted that the corresponding experiment can be omitted. For example, by omitting any one experiment, the K-efficient RCN is increased by at least an order of magnitude. However, as a counterexample, omitting the action potential propagation experiments has little effect on the D-efficient RCN. The goals of modeling and estimation should be carefully considered in selecting an optimality criterion.

In conclusion, there is a great need to develop, calibrate, and validate cardiac cell models and other types of models that are appropriate for use at multiple scales. Given the theoretical basis for the existing equations for electrical activity in the heart at multiple scales, it may

be feasible to develop and justify robust cardiac cell models that are locally indentifiable, make efficient use of experimental data, and are consistent with phenomenon at multiple scales.

6. SUPPLEMENTARY MATERIALS

The Code Supplement, Web Appendices, and Web Figures referenced in Sects. 4.1, 4.2, 4.3, 4.4, 4.7, and 4.8 are available with this paper.

ACKNOWLEDGEMENTS

This work was supported by NIH/NHLBI award "Optimal Design of Challenge-Response Experiments in Cardiac Electrophysiology" (1R01HL118392) and National Science Foundation Cyber Physical Systems Frontier Award "Foundation, Compositional, Approximate, and Quantitative Reasoning for Medical Cyber-Physical Systems" (Award Number: 1446832).

[Received July 2015. Accepted January 2016.]

REFERENCES

Beaumont, J., Roberge, F. A., and Leon, L. J. (1993). On the interpretation of voltage-clamp data using the Hodgkin-Huxley model. *Mathematical Biosciences* **115,** 65–101.

Berecki, G., Wilders, R., de Jonge, B., van Ginneken, A. C. G., and Verkerk, A. O. (2010). Re-evaluation of the action potential upstroke velocity as a measure of the Na^+ current in cardiac myocytes at physiological conditions. *PLoS One* **5**.

Csercsik, D., Hangos, K. M., and Szederkényi, G. (2012). Identifiability analysis and parameter estimation of a single Hodgkin-Huxley type voltage dependent ion channel under voltage step measurement conditions. *Neurocomputing* **77,** 178–188.

Fedorov, V. V. and Leonov, S. L. (2013). *Optimal Design for Nonlinear Response Models*. Chapman & Hall/CRC Biostatistics Series. Taylor & Francis.

Fink, M. and Noble, D. (2009). Markov models for ion channels: versatility versus identifiability and speed. *Philosophical Transactions of the Royal Society A* **367,** 2161–2179.

Gray, R. A., Mashburn, D. N., Sidorov, V. Y., and Wikswo, J. P. (2013). Quantification of transmembrane currents during action potential propagation in the heart. *Biophysical Journal* **104,** 268–278.

Grewal, M. S. and Glover, K. (1976). Identifiability of linear and nonlinear dynamical systems. *IEEE Transactions on Automatic Control* **21,** 833–836.

Hengl, S., Kreutz, C., Timmer, J., and Maiwald, T. (2007). Data-based identifiability analysis of non-linear dynamical models. *Bioinformatics* **23,** 2612–2618.

Hodgkin, A. L. and Huxley, A. F. (1952). A quantitative description of membrane current and its application to conduction and excitation in nerve. *Journal of Physiolgy* **117,** 500–544.

Hunter, P. J. and Borg, T. K. (2003). Integration from proteins to organs: the Physiome Project. *Nature Reviews Molecular Cell Biology* **4,** 237–243.

Ingram, C. D., Cameron, I. T., and Hangos, K. M. (2004). Classification and analysis of integrating frameworks in multiscale modelling. *Chemical Engineering Science* **59,** 2171–2187.

Jacquez, J. A. and Greif, P. (1985). Numerical parameter identifiability and estimability: Integrating identifiability, estimability, and optimal sampling design. *Mathematical Biosciences* **77,** 201–227.

Joyner, R. W., Ramza, B. M., Osaka, T., and Tan, R. C. (1991). Cellular mechanisms of delayed recovery of excitability in ventricular tissue. *American Journal of Physiology* **260,** H225–H233.

Kim, D. and Lindsay, B. G. (2014). Empirical identifiability in finite mixture models. *Annals of the Institute of Statistical Mathematics*.

Lee, J., Smaill, B., and Smith, N. (2006). Hodgkin-Huxley type ion channel characterization: An improved method of voltage clamp experiment parameter estimation. *Journal of Theoretical Biology* **242,** 123–134.

McLean, K. A. P. and McAuley, K. B. (2012). Mathematical modelling of chemical processes – obtaining the best model predictions and parameter estimates using identifiability and estimability procedures. *The Canadian Journal of Chemical Engineering* **90,** 351–366.

Raba, A. E., Cordeiro, J. M., Antzelevitch, C., and Beaumont, J. (2013). Extending the conditions of application of an inversion of the Hodgkin-Huxley gating model. *Bulletin of Mathematical Biology* **75,** 752–773.

Raue, A., Kreutz, C., Maiwald, T., Bachmann, J., Schilling, M., Klingmüller, U., and Timmer, J. (2009). Structural and practical identifiability analysis of partially observed dynamical models by exploiting the profile likelihood. *Bioinformatics* **25,** 1923–1929.

Rempel, M. F. and Zhou, J. (2014). On exact K-optimal designs minimizing the condition number. *Communications in Statistics - Theory and Methods* **43,** 1114–1131.

Rothenberg, T. J. (1971). Identification of parametric models. *Econometrica* **39,** 577–591.

Walter, E. and Pronzato, L. (1996). On the identifiability and distinguishability of nonlinear parametric models. *Mathematics and Computers in Simulation* **42,** 125–134.

Wang, G. J. and Beaumont, J. (2004). Parameter estimation of the Hodgkin-Huxley gating model: An inversion procedure. *SIAM Journal on Applied Mathematics* **64,** 1249–1267.